

## Mapping surrogate gasoline compositions into RON/MON space

Neal Morgan <sup>a</sup>, Andrew Smallbone <sup>b</sup>, Amit Bhave <sup>b</sup>, Markus Kraft <sup>a,\*</sup>, Roger Cracknell <sup>c</sup>, Gautam Kalghatgi <sup>c</sup>

<sup>a</sup> Department of Chemical Engineering, University of Cambridge, Cambridge CB2 3RA, United Kingdom

<sup>b</sup> Reaction Engineering Solutions Ltd., 61 Canterbury Street, Cambridge CB4 3QG, United Kingdom

<sup>c</sup> Shell Global Solutions, Shell Technology Centre Thornton, P.O. Box 1, Chester CH1 3SH, United Kingdom

### ARTICLE INFO

#### Article history:

Received 5 August 2009

Received in revised form 7 January 2010

Accepted 8 February 2010

Available online 2 March 2010

#### Keywords:

RON

MON

Fuel sensitivity

Surrogate gasolines

Modelling

### ABSTRACT

In this paper, new experimentally determined octane numbers (RON and MON) of blends of a tri-component surrogate consisting of toluene, n-heptane, i-octane (called toluene reference fuel TRF) arranged in an augmented simplex design are used to derive a simple response surface model for the octane number of any arbitrary TRF mixture. The model is second-order in its complexity and is shown to be more accurate to the standard "linear-by-volume" (LbV) model which is often used when no other information is available. Such observations are due to the existence of both synergistic and antagonistic blending of the octane numbers between the three components. In particular, antagonistic blending of toluene and iso-octane leads to a maximum in sensitivity that lies on the toluene/iso-octane line. The model equations are inverted so as to map from RON/MON space back into composition space. Enabling one to use two simple formulae to determine, for a given fuel with known RON and MON, the volume fractions of toluene, n-heptane and iso-octane to be blended in order to emulate that fuel. HCCI engine simulations using gasoline with a RON of 98.5 and a MON of 88 were simulated using a TRF fuel, blended according to the derived equations to match the RON and MON. The simulations matched the experimentally obtained pressure profiles well, especially when compared to simulations using only PRF fuels which matched the RON or MON. This suggested that the mapping is accurate and that to emulate a refinery gasoline, it is necessary to match not only the RON but also the MON of the fuel.

### 1. Introduction

The drive to produce ever more efficient forms of internal combustion engine is requiring a greater symbiotic relationship between the engine and the fuel that burns within it. In particular, the fuel's resistance to auto-ignition (or propensity to autoignite) is an important characteristic which can, to a large part, dictate the ability of an engine to work to its full thermodynamic potential. In a compression-ignition (CI) engine, one wishes the fuel to ignite rapidly after injection into the combustion chamber. In a spark-ignition (SI) engine however, a high resistance to auto-ignition is favoured as the main limiting factor of thermodynamic efficiency is "knocking"—an unwanted ringing sound caused by auto-ignition (which can lead to serious engine damage) of the fuel/air mixture ahead of the turbulent flame front (called the "end-gas").

For some 70 years now, the measure by which a fuel's resistance to knock is characterised has been the octane number (ON). These are measured under two differing engine conditions in a standard "Cooperative Fuels Research" (CFR) Engine. The two conditions produce two octane numbers: the research

octane number (RON) [1], and the motor octane number (MON) [2]. The fuel's RON (or MON) is measured by inducing "maximum" knock using the test fuel by adjusting some parameters (dependent on the test) of the engine, then finding a blend of n-heptane and i-octane (2,2,4 trimethyl pentane) – known as primary reference fuel (PRF) – which matches that knocking behaviour. The volume percentage of i-octane in the reference fuel then tells one the ON of that fuel.

In general, a refinery-blended gasoline will have a higher RON than its corresponding MON, the difference being denoted the "fuel sensitivity" (S):

$$S = RON - MON. \quad (1)$$

The reason has been alluded to the "negative temperature coefficient" (NTC) region in the ignition delay curves of paraffinic (and hence primary reference fuels [3]) which means that paraffinic fuels are more resistant to auto-ignition at the temperatures and pressures associated with the MON test than real fuels. Actual gasolines contain a mixture of n-, i- and cyclo-paraffins, olefins, and aromatics, the latter three of which do not tend to possess such a strong NTC region (if, indeed, any at all). Hence, under the MON test, paraffinic fuels are more resistant to auto-ignition and hence have higher MON numbers.

\* Corresponding author.

E-mail address: [mk306@cam.ac.uk](mailto:mk306@cam.ac.uk) (M. Kraft).

The fact that real gasoline exhibits fuel sensitivity is of critical importance to future engine technologies [4]. In particular, there is strong evidence that as engines become boosted (turbocharged) and “downsized”, the true auto-ignition resistance of the fuel shifts from its RON or MON to another value known as its Octane Index (OI). The Octane Index is defined by

$$OI = RON - K \cdot S, \quad (2)$$

where  $K$  is a constant which is dependent only on the engine conditions. By definition,  $K = 0$  for the RON condition and  $K = 1$  at the MON condition. One can see that as  $K$  becomes negative, it is possible for a sensitive fuel to have an OI greater than its RON. This has major implications for the way that future engines could make the best possible use of the refinery blended fuels available – benefits including greater efficiency and power, arising from the fact that the engine can be run at its most efficient spark timing for more of its operating window.

With this in mind one can see that to successfully model a gasoline fuel in current and future engines, one needs to be able to simulate a fuel with a RON different to its MON. This is simply impossible to do with the PRF models used traditionally. Toluene reference fuels (TRFs) – ternary mixtures of toluene, n-heptane and i-octane – possess inherent fuel sensitivity and have gone some way to help us develop simple gasoline surrogate models which capture the important combustion metrics [5,6]. The question for engine combustion modellers then becomes: “Is a surrogate fuel model which can re-create the RON and MON properties of a real gasoline sufficient for modelling the combustion of any real fuel?” In order to answer that, one requires a way to determine the RON and MON of a particular mixture, and vice-versa – to mimic a fuel with a given RON and MON, how should one blend up the surrogate fuel?

While for a PRF there is a direct and concrete link between fuel composition and the ON, for ternary TRF blends no such link exists. Without experimental data, in practice “linear-by-volume” (LbV) models are the only means of how to estimate the RON and MON of tri-component blends, however this can introduce errors, especially when one knows that there may be synergistic or antagonistic blending of properties between components.

The purpose of this paper is therefore to address the problem using a 2nd order response surface model [7] to map the toluene/n-heptane/i-octane space with respect to RON and MON (and hence Sensitivity), and then use this fit to allow one to determine the RON and MON for any TRF surrogate. This would allow the research community to refer to surrogate fuels in a manner which would be more beneficial to industry (i.e. in terms of RON and MON). The second purpose of the paper is to use the above methodology to further validate a recently published TRF mechanism [6] within the framework of a stochastic reactor model (SRM) [8] to simulate HCCI combustion of a non-reference fuel of known RON and MON [9].

## 2. Experimental

### 2.1. Procedure and design

When compared to a shock-tube experiment for the determination of an ignition delay time, or a combustion bomb experiment to elucidate the laminar flame speed of a fuel, the RON and MON tests can seem somewhat abstract. Both tests make use of the CFR engine which has a variable compression ratio (CR), a fuel metering system which easily adjusts the fuel-air ratio ( $\phi$ ), and a “knock meter” which gives a value of the “knocking intensity” based on the pressure rise rate in arbitrary units between 0 and 100. The pressure rise rate is measured using a “detonation” (the term taken from directly from the test procedures [1,2] albeit an incorrect def-

**Table 1**  
 Physical dimensions of the CFR engine for RON and MON tests.

Bore (mm)	82.6
Stroke (mm)	114.3
Displacement (cm <sup>3</sup> )	611.7
Connecting rod length (mm)	265.2
Compression ratio	4:1–18:1
Inlet valve opening (IVO) (CAD BTDC)	350
Inlet valve closing (IVC) (CAD BTDC)	146
Exhaust valve opening (EVO) (CAD ATDC)	140
Exhaust valve closing (EVC) (CAD ATDC)	375

**Table 2**  
 Test conditions for the RON test.

Intake temperature (°C)	52
Engine speed (RPM)	600
Spark timing (CAD BTDC)	13

ition based on the observations of [10]) pickup which is a magnetostrictive-type transducer fixed to the engine cylinder. The dimensions of the engine are given in Table 1.

The RON test is run under the engine conditions laid out in Table 2.

The procedure to determine the octane number is described below:

1. *Calibrating the knock meter:* A reference fuel with ON thought to be close to that of the test fuel is introduced into the engine and the compression ratio is adjusted according to tables such that knocking is induced. The fuel level (air-fuel ratio) is adjusted to give maximum knock intensity (KI) and the knock meter gain is adjusted to give a reading of  $50 \pm 2$ .
2. *Initial estimation of test fuel's ON:* The test fuel is introduced into the engine and the compression ratio adjusted to achieve a “mid-scale” knock meter reading. The fuel level (air-fuel ratio) is adjusted to give maximum KI and then the compression ratio is adjusted so that the knock reading is  $50 \pm 2$ . This meter reading is recorded ( $KI_{test}$ ) and the compression ratio used to estimate the ON of the fuel.
3. *Selection of PRFs for comparison:* Two PRF fuels, one with an ON slightly higher and the other with an ON slightly lower than the test fuel are prepared (the difference between the fuels is dependent on the estimated ON of the test fuel).
4. *Determining the KI of the first PRF:* The first PRF fuel is introduced to the engine and the fuel level (air-fuel ratio) adjusted to give maximum knock intensity which is then recorded ( $KI_{PRF-L}$ ).
5. *Determining the KI of the second PRF:* The second PRF fuel is introduced to the engine and the fuel level (air-fuel ratio) adjusted to give maximum knock intensity which is then recorded ( $KI_{PRF-H}$ ).

Using the three readings for knock intensity,  $KI_{test}$  for the test fuel,  $KI_{PRF-L}$  for the lower PRF fuel, and  $KI_{PRF-H}$  for the higher PRF fuel and the octane numbers of the PRF fuels, the octane number for the test fuel is determined by linear interpolation using the formula below

$$ON_{test} = ON_{PRF-L} + \left( \frac{KI_{PRF-L} - KI_{test}}{KI_{PRF-L} - KI_{PRF-H}} \right) + (ON_{PRF-H} - ON_{PRF-L}). \quad (3)$$

The MON test procedure is identical to the RON test procedure however the test conditions are subtly different as shown in Table 3.

Note that the spark timing is inversely proportional to the cylinder height and proportional 1/CR (highest cylinder height  $\rightarrow 26^\circ$  BTDC, lowest cylinder height  $\rightarrow 14^\circ$  BTDC).

**Table 3**  
 Test conditions for the MON test.

Intake temperature (°C)	149
Engine speed (RPM)	900
Spark timing (CAD BTDC)	26–14

Ten blends of toluene, i-octane and n-heptane were created according to an augmented simplex experimental design for mixtures. The design points in  $n$ -dimensions (in this case  $n = 3$ ) are arranged in such a way as to reduce variance bias in the estimation of the coefficients of a polynomial function which is fitted to the results of the experiments. This was all done according to Response Surface Methodology (RSM) [7] which is a collection of statistical and mathematical techniques which combines experimental design with rigorous regression of polynomial “surfaces” onto those design points.

The TRF blends were made up from high-grade (>99.75% purity) component chemicals in accordance with the ASTM standards, and the octane numbers found according to the test procedures above (see [1] and [2] for more details).

## 2.2. Results

The blend compositions are presented in Table 4 along with the corresponding RON and MON numbers determined using the above procedures for those blends.

## 3. Fitting response surfaces

The results from the previous section were used to fit various forms of response surface such that a simple mapping could be established between blend composition and octane number.

### 3.1. The linear-by-volume (LbV) model

The simplest mixing model for tri-component blends is the linear-by-volume, LbV, model. This is simply a sum of the contributions of the three components weighted by their volume fractions, denoted  $x_i$  – Note that  $x$  is not used to denote mole fraction. With respect to the TRF blends, the equation can be written as

$$RON = a_{tol}x_{tol} + a_{iO}x_{iO} + a_{nH}x_{nH}, \quad (4)$$

where the  $a$ s represent the coefficients for toluene ( $tol$ ), i-octane ( $iO$ ) and n-heptane ( $nH$ ), and are equal to 120, 100 and 0 respectively. For the corresponding MON equation the constants would be  $a_{tol} = 109$ ,  $a_{iO} = 100$  and  $a_{nH} = 0$ . The coefficients for sensitivity would simply be the difference between the RON and MON coefficients.

**Table 4**

Experimental design points for the tri-component mixtures with corresponding experimentally derived octane numbers.

Toluene (vol.%)	i-Octane (vol.%)	n-Heptane (vol.%)	RON	MON
100.0	0.0	0.0	120.0	109.0
66.6	16.6	16.6	98.0	87.4
50.0	50.0	0.0	110.0	99.3
50.0	0.0	50.0	65.9	57.7
33.3	33.3	33.3	76.2	70.9
16.6	66.6	16.6	87.0	84.0
16.6	16.6	66.6	39.0	37.0
0.0	100.0	0.0	100.0	100.0
0.0	50.0	50.0	50.0	50.0
0.0	0.0	100.0	0.0	0.0

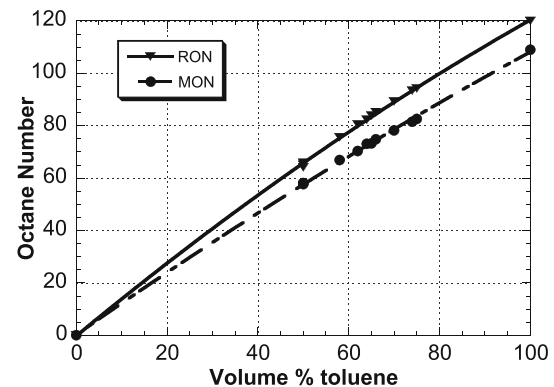


**Fig. 1.** Octane number vs. vol.% toluene for toluene/n-heptane blends with quadratic lines of best fit.

### 3.2. Second order model (O2M)

As mentioned earlier, LbV models lack any ability to describe antagonistic or synergistic blending. This is of concern, especially when there is clear evidence that the blending of certain components – take for example toluene and n-heptane – is non-linear (see Fig. 1). To redress this, one may wish to use a 2nd order model which includes parameter interaction.

The full 2nd order model (denoted O2M) for this particular system can be written as

$$RON = a_{tol}x_{tol} + a_{iO}x_{iO} + a_{nH}x_{nH} + a_{tol,iO}x_{tol}x_{iO} + a_{iO,nH}x_{iO}x_{nH} + a_{tol,nH}x_{tol}x_{nH} + a_{tol,iO,nH}x_{tol}x_{iO}x_{nH}, \quad (5)$$

where the coefficients  $a_{tol}$ ,  $a_{iO}$  and  $a_{nH}$  are the same as with Eq. (4),  $a_{tol,iO}$ ,  $a_{iO,nH}$ ,  $a_{tol,nH}$  are the coefficients for the binary-interaction terms, and  $a_{tol,iO,nH}$  is the coefficient for the ternary interaction term. The binary interaction coefficients are found by multiplying the deviations from linear behaviour at the three 1:1 blends by 4, whilst the ternary interaction term is found by multiplying the 1:1:1 blend's deviation from linearity by 27 (see [7] for more details).

### 3.3. The modified linear-by-volume (MLbV) model

One could think of all the blends considered as consisting of toluene blended with a certain ‘strength’ PRF. As such, it would be useful to define the model equations in terms of PRF and toluene volume fraction. We will define a variable,  $p$ , which is simply a renormalisation of PRF from [0,100] to [0,1], and by using the identity for  $p$ :

$$p = \frac{x_{iO}}{x_{iO} + x_{nH}}, \quad (6)$$

and using the fact that  $a_{nH} = 0$ , one can re-write Eq. (4) as

$$RON = a_{tol}x_{tol} + a_{iO}p - a_{iO}x_{tol}p. \quad (7)$$

Note that  $p$  is undefined when  $x_{tol} = 1$  which could lead to unwanted behaviour of the equation. As such we will prescribe that when  $x_{tol} = 1$ ,  $p = 0$ .

In addition to response surface Eqs. (4) and (5), a third equation will be defined, the Modified Linear by Volume (denoted MLbV) equation, which is more simple than the full 2nd order equation but still contains a non-linear blending term:

$$RON = a_p p + a_{tol}x_{tol} + a_{tol}^2 x_{tol}^2 + a_{tol,p}x_{tol}p. \quad (8)$$

The coefficients for this model were fitted to the 10-point experimental design in Table 4 using a least-squares technique.

**Table 5**  
 Coefficients for the LbV response surface model for RON, MON and Sensitivity.

Coefficient	$a_{tol}$	$a_{iO}$	$a_{nH}$
RON	120	100	0
MON	109	100	0
Sensitivity	11	0	0

**Table 6**  
 Coefficients for the 2nd order response surface models for RON, MON and Sensitivity.

Coefficient	$a_{tol}$	$a_{iO}$	$a_{nH}$	$a_{tol,iO}$	$a_{iO,nH}$	$a_{tol,nH}$	$a_{tol,iO,nH}$
RON	120	100	0	0	0	23.6	77.3
MON	109	100	0	0	-20.8	12.8	33.3
Sensitivity	11	0	0	0	20.8	10.8	44.0

**Table 7**  
 Coefficients for the modified LbV response surface model for RON, MON and Sensitivity.

Coefficient	$a_p$	$a_{tol}$	$a_{tol^2}$	$a_{tol,p}$
RON	100	142.79	-22.651	-111.95
MON	100	128.00	-19.207	-119.24
Sensitivity	0	14.79	-3.444	7.29

The coefficients for Eqs. (4), (5) and (8) are presented in Tables 5–7 respectively.

### 3.4. Validation of the response surface models

The models were fitted using the data in Table 4 and were then validated against other known values of RON and MON that could be found in the literature for these ternary mixtures. This validation data is presented in Table 8.

The three models were used to calculate RON and MON for each of the  $N$  data points presented. Their sum of squared errors, calculated using

$$SSE = \sum_{i=1}^N (RON_{expt,i} - RON_{calc,i})^2, \quad (9)$$

**Table 8**  
 Experimentally determined RON and MON data for ternary mixtures of toluene, n-heptane and i-octane.

Toluene (vol.%)	i-Octane (vol.%)	n-Heptane (vol.%)	PRF	RON	MON	S	Refs.
50	0	50	0.0	65.1	58.0	7.1	[1,2]
58	0	42	0.0	75.6	66.9	8.7	[1,2]
66	0	34	0.0	85.2	74.8	10.4	[1,2]
74	15	11	57.7	103.3	92.6	10.7	[1,2]
74	20	6	76.9	107.6	96.6	11.0	[1,2]
74	26	0	100.0	113.0	100.8	12.2	[1,2]
70	0	30	0.0	89.3	78.2	11.1	[1,2]
74	0	26	0.0	93.4	81.5	11.9	[1,2]
74	5	21	19.2	96.9	85.2	11.7	[1,2]
74	10	16	38.5	99.8	88.7	11.1	[1,2]
100	0	0	0.0	120.0	109.0	11.0	[27]
65	0	35	0.0	83.9	73.2	10.7	[28]
64	0	36	0.0	82.3	73.1	9.2	[29]
62	0	38	0.0	80.5	70.3	10.2	[28]
50	0	50	0.0	64.1	58.1	6.0	[29]
75	0	25	0.0	94.2	82.6	11.6	[28]
20	63	17	78.8	88.0	85.0	3.0	[6]
14	69	17	80.2	87.0	85.0	2.0	[6]
66.7	16.7	16.7	50.0	98.0	87.4	10.6	This work
16.7	16.7	66.7	20.0	39.0	37.0	2.0	This work
16.7	66.7	16.7	80.0	87.0	84.0	3.0	This work
50.0	0.0	50.0	0.0	65.9	57.7	8.2	This work
50.0	50.0	0.0	100.0	110	99.3	10.7	This work
33.3	33.3	33.3	50.0	76.2	70.9	5.3	This work

**Table 9**  
 SSE analysis of the three response surface models for RON and MON.

	LbV	$\mathcal{O}2M$	MLbV
RON	352.3	59.9	15.7
MON	188.8	38.4	73.0
Sensitivity	186.2	58.4	60.3
Total	727.4	156.7	149.1

were tabulated – the results of this analysis are presented in Table 9. One can see that the LbV model introduces significant errors when compared to the  $\mathcal{O}2M$  model or the MLbV model. Given its relative simplicity with respect to the number of free parameters, and its lowest overall SSE, the MLbV model will be used for the rest of this paper.

Figs. 2–4 show the response surfaces for RON, MON and Sensitivity respectively in the tri-component mixture space. The curvature

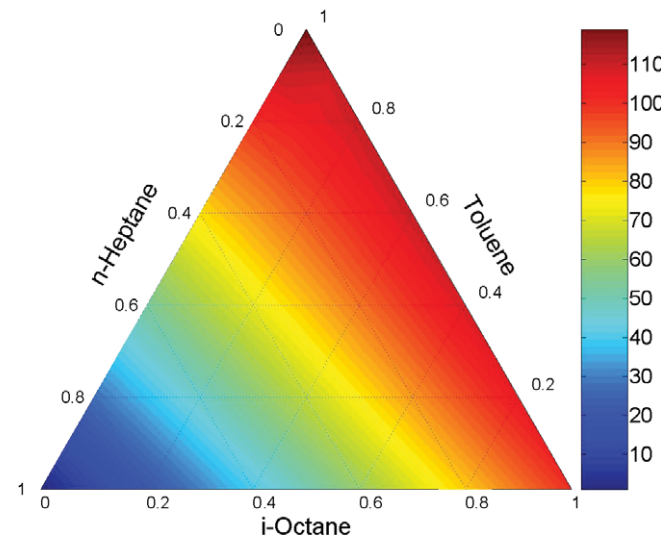


**Fig. 2.** A contour plot of RON in the tri-component mixture space generated using the 3-parameter MLbV model.

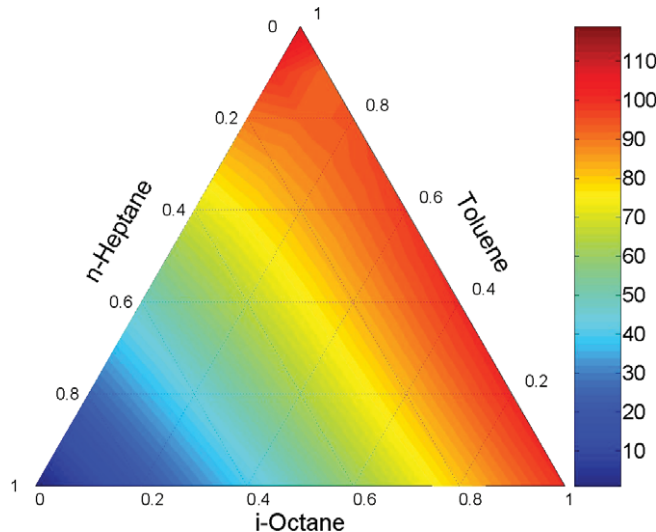


**Fig. 3.** A contour plot of MON in the tri-component mixture space generated using the 3-parameter MLbV model.

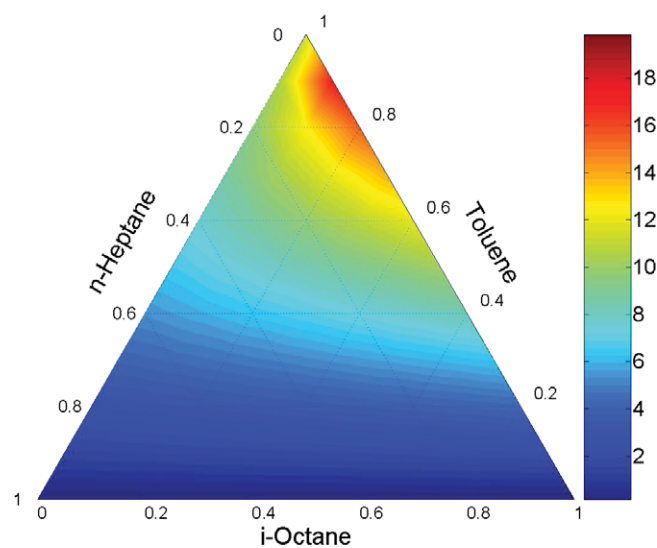


**Fig. 4.** A contour plot of sensitivity in the tri-component mixture space generated using the 3-parameter MLbV model.

of the contours shows that there is some degree of non-linearity in the blending of the components, and the shape of the sensitivity contours in Fig. 4 show that there is clearly some antagonistic blending between toluene and i-octane.

### 3.5. Inverting the equations

Now that there exists a mapping from the ternary mixture space of toluene/n-heptane/i-octane into RON/MON/Sensitivity space, it would be useful from an engineering point of view to be able to reverse this, i.e. answer the question: “which composition of fuel should be used in order to emulate a specified RON & MON?”.

Eq. (8) for RON can be rearranged to give

$$p = \frac{RON - (a_{tol}x_{tol} + a_{tol}^2x_{tol}^2)}{100 + a_{tol,p}x_{tol}}, \quad (10)$$

which can then be substituted into the MLbV equation for Sensitivity to give

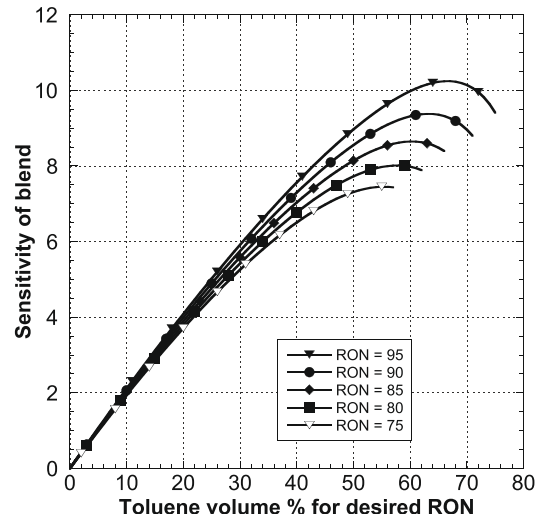


**Fig. 5.** Curves of toluene vol.% vs. Sensitivity (RON-MON) for a required RON.

$$\begin{aligned} \text{Sensitivity} = & a_{S,tol}x_{tol} + a_{S,tol}^2x_{tol}^2 \\ & + \frac{a_{S,tol,p}x_{tol}(RON - a_{R,tol}x_{tol} - a_{R,tol}^2x_{tol}^2)}{100 + a_{R,tol,p}x_{tol}^2}, \end{aligned} \quad (11)$$

where the extra initial subscripts on the coefficients (R or S) refer to the “RON” or “Sensitivity” coefficients to use.

With these two equations, one is now in a position to calculate the composition of a mixture with a specified RON and Sensitivity (and hence MON). Fig. 5 shows how the Sensitivity of fuels with specified RONs change with varying toluene content. Hence, for a given RON and Sensitivity, one now knows how much toluene should be in that blend. Fig. 6 subsequently shows how strong the PRF that is to be blended with the toluene needs to be to attain the specified attributes.

It is interesting to note that for some of the higher RON fuels ( $RON > 80$ ) with high fuel sensitivity ( $S > 8$ ), there appears to exist two compositions which satisfy the RON, MON and Sensitivity requirements. This could arise because of the form of the equation that was chosen for the fit. However, since it is known that there exists some antagonistic blending behaviour between toluene and i-octane for MON, and synergistic blending between toluene and n-heptane for RON and MON, there might also be a chemical

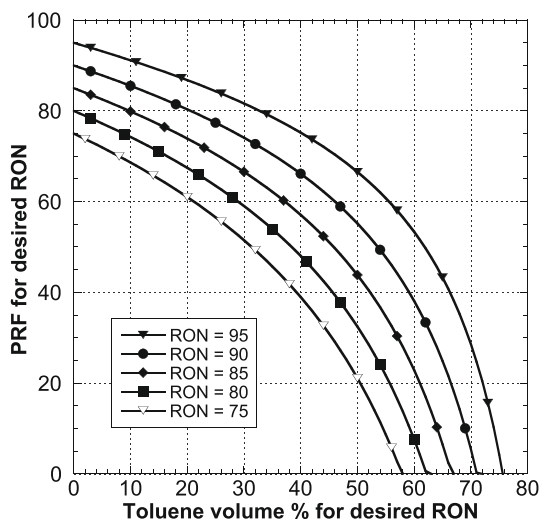


**Fig. 6.** Curves of toluene vol.% vs. the PRF strength to be added for a required RON.

**Table 10**

Compositions of two fuel blends with RON = 95 and MON = 85 according to the fitted blending equation.

Fuel no.	Toluene (vol.%)	i-Octane (vol.%)	n-Heptane (vol.%)
1	60.537	20.645	18.818
2	71.366	6.598	22.036

**Table 11**  
 Representative "RON" and "MON" conditions for chemical kinetic simulations.

Operating point	Pressure (bar)	Temperature (K)	$\phi$ (-)
"RON-like"	23.0	800	1.0
"MON-like"	20.0	900	1.0

explanation for the duality of solutions. To confirm this, more experiments around these points should be performed.

Two octane numbers which are of particular interest to engine modellers are: RON = 95, MON = 85. These correspond to the minimum British and European standard, EN-228 [11] for the RON and MON of a gasoline fuel. From the equations derived above, there appear to be two blends which satisfy these specifications. Their compositions are shown in Table 10.

#### 4. Simulations

##### 4.1. Chemical kinetics

In order to gain further insight into the sources of antagonistic blending behaviour noted in RON and MON for the tri-component blends, a series of sensitivity tests were carried out using an in-house chemical solver operated in homogenous reactor mode similar to that described by [8]. The chemical kinetics were modelled using a semi-detailed reaction mechanism for TRF oxidation [6] which contains 137 species. This fuel model has been validated against a wide variety of experimental data, from shock tubes and rapid compression machines for ignition delay times, to combustion bomb data for laminar flame speeds.

Two computations considered representative of the RON and MON tests were adopted, the key boundary conditions for these

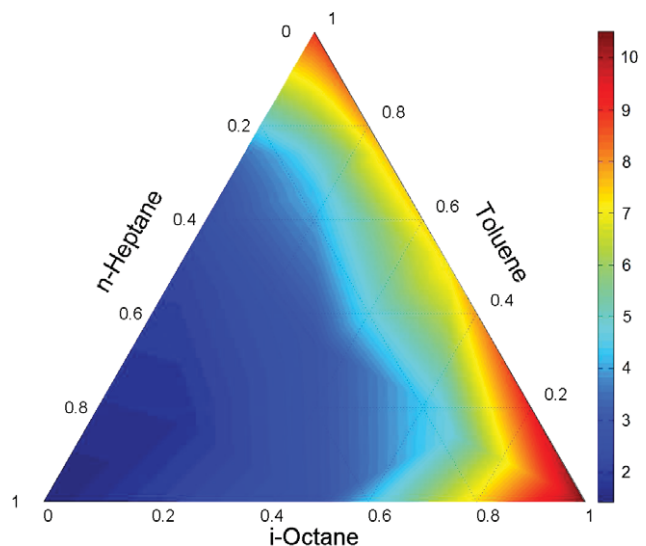


**Fig. 8.** A contour plot of ignition delay times in ms at the representative "MON-like" condition in the tri-component mixture space generated using the 3-parameter MLbV model.

are given in Table 11. Resulting ignition delay times from these computations are presented as "RON-like" and "MON-like" conditions in Figs. 7 and 8 respectively.

Bearing in mind that in the actual octane tests, the progress of auto-ignition chemistry is facilitated by the preceding pressure-temperature history driven by the compression of the end gas by both piston and an expanding propagating flame front, that therefore these auto-ignition events are (at least in part) coupled to the corresponding turbulent flame speed [12]. When the corresponding ignition delay times are compared with the actual RON and MON experiments in Figs. 2 and 3 respectively, the main trends of concave lines of constant "auto-ignition" behaviour in terms of RON, MON or here the ignition delay are observed, particularly at higher octane numbers. This suggests that these ignition delay compactations are still sensitive to those same key reactions which are responsible for the non-linear responses noted in the RON and MON tests.

In order to identify the sources of these behaviour, further analysis of the main cross-over reactions was carried out using a modified sensitivity analysis at both the "RON-like" and "MON-like" conditions. A measure of the non-linearity of the octane numbers was defined as the difference between the computed ignition delay times and those determined directly on the basis of a linear-by-volume, LbV blending model by calculating the residual

$$R^2 = (\tau - \tau_{LbV})^2. \quad (12)$$

In this formula, where  $\tau$  is the ignition delay time determined from the mechanism and  $\tau_{LbV}$  is the ignition delay time calculated on a linear-by-volume, LbV basis i.e.

$$\tau_{LbV} = (\tau_{iO}x_{iO}) + (\tau_{nH}x_{nH}) + (\tau_{tol}x_{tol}), \quad (13)$$

where  $\tau_{iO}$ ,  $\tau_{nH}$  and  $\tau_{tol}$  are the computed ignition delay times for pure i-octane, n-heptane and toluene respectively and  $x$  are their respective mixture volume fractions.

The ignition delay times were determined for 1% deviations in the reaction rate,  $k$  or more specifically the pre-exponent factor,  $A$  for the cross-over reactions,  $r$  in the mechanism. Their corresponding residuals,  $R_r$  were then computed. The sensitivity of the reaction with respect to the residual,  $S_r$  was determined as below.

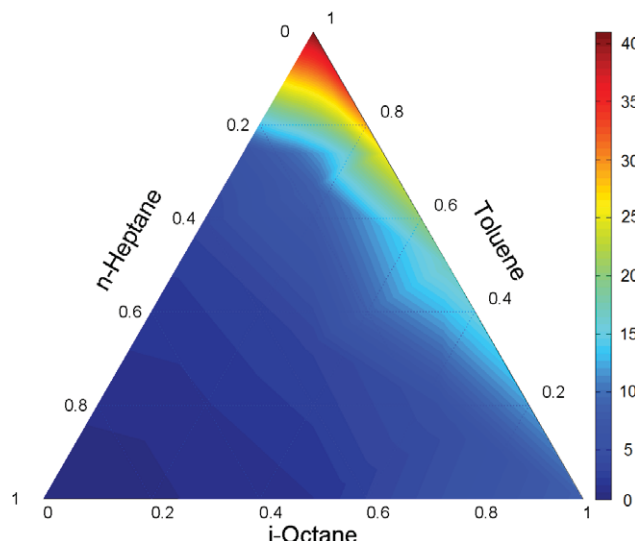


**Fig. 7.** A contour plot of ignition delay times in ms at the representative "RON-like" condition in the tri-component mixture space generated using the 3-parameter MLbV model.

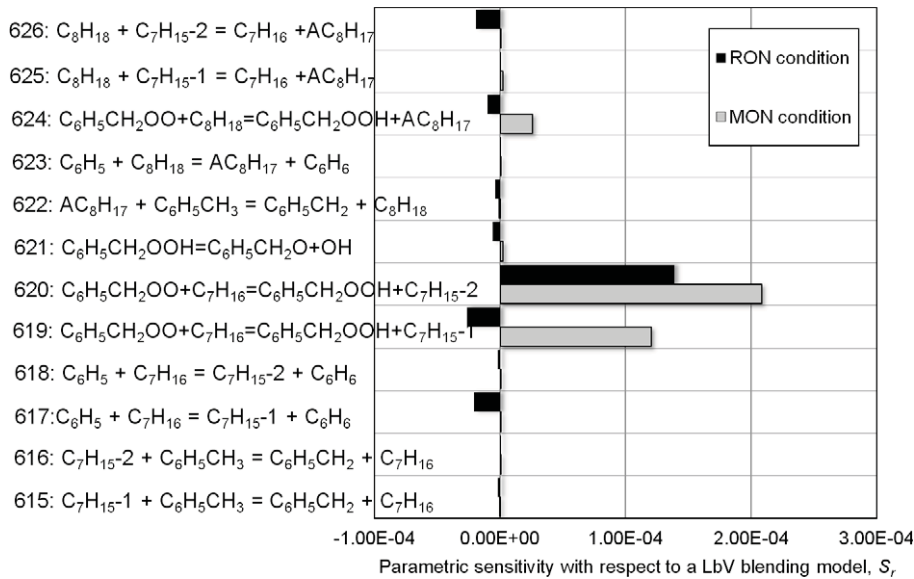


Fig. 9. Parametric sensitivities with respect to a LbV blending model for all cross-over reactions.

$$S_r = \frac{R_r - R_0}{k_r - k_0}, \quad (14)$$

where  $R_0$  is the residual obtained with zero deviation. This was carried out for both the “RON-like” and “MON-like” conditions for all TRF blends over the whole mixture space with results presented in Fig. 9.

As presented, reaction no. 620 is the most significant source of the observed antagonistic blending, through the formation of a benzylperoxy radical from toluene. To demonstrate in which compositions this reaction is most active, corresponding local sensitivities are presented in Figs. 10 and 11.

These diagrams demonstrate the impact of reaction 620 at the “RON-like” and “MON-like” conditions over the complete mixture space, this reaction proved most active at higher i-octane and toluene concentrations and thus in the same mixture spaces in which most antagonistic blending is reported, suggesting its influence is the most significant source of the reported antagonistic blending.

#### 4.2. Engine

In order to further assess the validity of the response surface model for selecting the appropriate composition of TRF blend when emulating a gasoline fuel, simulations were performed using a stochastic reactor model (SRM) code and a TRF kinetic mechanism to model an engine running in HCCI mode.

In the past, the SRM code has been successfully employed in a number of studies of port fuel injected HCCI combustion [13], alternative fuel blends [14], single early direct injection HCCI [15], dual injection HCCI [16], multi-cycle transient simulation and control [17–19], soot formation [20], and has been coupled to the computational fluid dynamics (CFD) code KIVA [21]. The SRM is employed to simulate the internal mixing and chemical processes in the combustion chamber, along with heat transfer to the cylinder walls. The model is preferable to conventional homogeneous reactor models for modelling HCCI combustion as it ac-

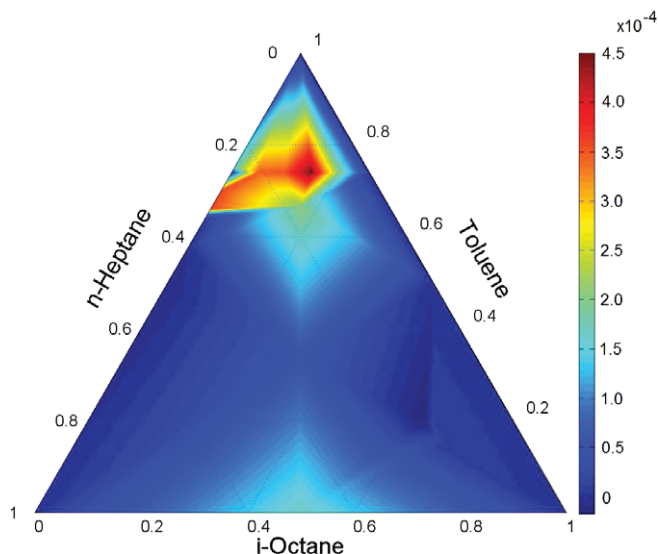


Fig. 10. Local parametric sensitivities with respect to a LbV blending model of reaction 620:  $C_6H_5CH_2OO + C_7H_{16} = C_6H_5CH_2OOH + C_7H_{15}-2$  at “RON-like” condition.

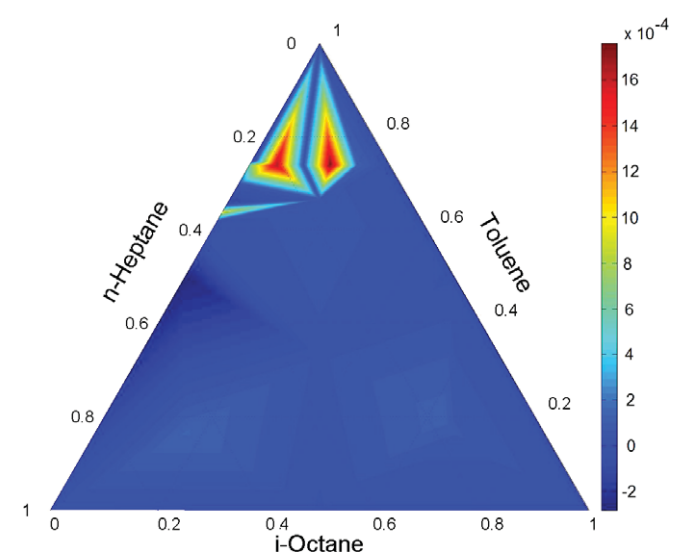
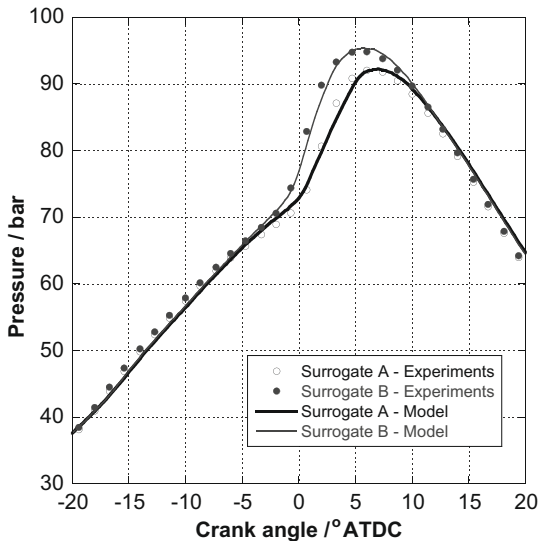


Fig. 11. Local parametric sensitivities with respect to a LbV blending model of reaction 620:  $C_6H_5CH_2OO + C_7H_{16} = C_6H_5CH_2OOH + C_7H_{15}-2$  at “MON-like” condition.



**Fig. 12.** Pressure curves from the validation study of Surrogate A comprised of 63% i-octane/17% n-heptane/20% toluene and Surrogate B comprised of 69% i-octane/17% n-heptane/14% toluene, an engine with bore = 86 mm, stroke = 86 mm, con-rod length = 143.5 mm, CR = 14.0.

counts for temperature and mixture inhomogeneities which are important in smoothing out the heat release rate. CPU times were of the order one hour which, while longer than homogeneous combustion models (taking of the order one minute), is considerably shorter than if a computational fluid dynamics (CFD) code were coupled even with vastly simplified chemistry.

#### 4.2.1. Chemical kinetic mechanism validation against engine data

Whilst during the mechanism development process significant validation was carried out against flame speeds [5], ignition delays times and some limited HCCI engine experiments [6], further confidence was attained by carrying out a more comprehensive validation study with HCCI engine experiments [22]. This was completed using the SRM for a range of i-octane/n-heptane, toluene/n-heptane and toluene/i-octane/n-heptane blends in two engines over a total of seven operating points. Key model parameters such as stochastic heat transfer coefficient and turbulent mixing times were fixed throughout, whilst initial mixture pressures, temperatures and equivalence ratios,  $\phi$  were derived from the experiments themselves. Generally, the model proved very robust typically yielding 50% heat release times to within  $\pm 2.0$  crank angle degrees. An example of model performance compared to experiment from the validation study is presented in Fig. 12. Here the model captures the ignition onset time as well as the heat release profiles very well thus developing further confidence firstly, in the adoption of the SRM for such applications and secondly, in the employed mechanism.

#### 4.2.2. Model application to a practical fuel

Having successfully validated the model, simulations were compared with experimental data obtained from a Volvo TD100 engine operated in HCCI mode using a typical practical high-octane gasoline fuel [9]. The engine dimensions are shown in Table 12 and the inlet conditions for three cases where the compression ratio (CR) and inlet temperature of the engine is changed are shown in Table 13.

The fuel used was a high-octane gasoline (Grön 98 MK1) with a RON of 98.5 and a MON of 88. The inverse equations (Eqs. (10) and (11)) were used to calculate the composition of the TRF mixture that would have the same RON and MON as the gasoline. Two

**Table 12**

Physical dimensions and test conditions of the Volvo TD100 engine for the gasoline HCCI experiment.

Bore (mm)	120.6
Stroke (mm)	140.0
Displacement (cm <sup>3</sup> )	1600
Connecting rod length (mm)	260.0

**Table 13**

Test conditions for the HCCI tests.

Case no.	CR	Intake temperature (°C)	Intake pressure (bar)	Engine speed (RPM)	$\lambda$
1	22.4	30	1.01	1000	3.0
2	20	70	1.01	1000	3.0
3	17.7	110	1.01	1000	3.0

**Table 14**

Composition of surrogate fuel blends with RON = 98.5 and MON = 88.

Fuel	RON	MON	Toluene (vol.%)	i-Octane (vol.%)	n-Heptane (vol.%)
TRF	98.5	88.0	75.418	5.833	18.749
PRF	98.5	98.5	0.000	98.500	1.500
PRF	88.0	88.0	0.000	88.000	12.000

PRF blends which matched the RON and MON of the gasoline separately were also emulated. The compositions of the fuels are shown in Table 14.

The cylinder pressure profiles for the experiments and simulations are shown in Figs. 13–15. As one can see, the TRF fuel accurately captured the timing of the main heat release event just after TDC for all three cases. By comparison, the 98.5 ON PRF fuel was much too resistant to auto-ignition at these particular engine conditions, and in the milder conditions (CR = 17.7 and 20), it did not ignite at all. The 88 ON fuel ignited far too easily for the CR = 22.4 and 20 cases but ignited at a similar time to the gasoline and TRF fuel in the CR = 17.7 case.

This suggests that in cases #1 and #2 the OI for the gasoline fuel is somewhere between its RON and MON, implying that the K-value for these experiments lie somewhere between 0 and 1. For case #3 however the ON of the gasoline was almost exactly the same as

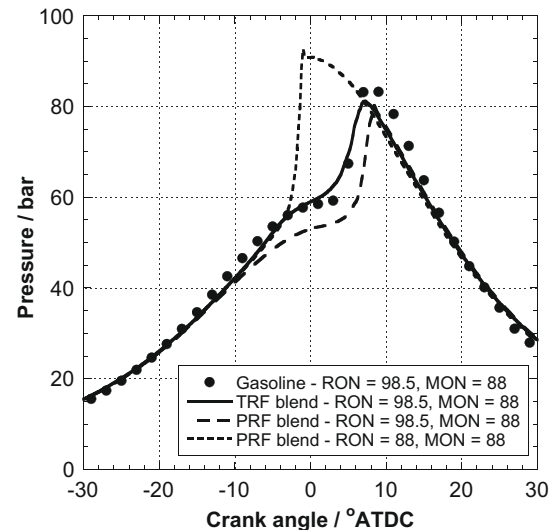


**Fig. 13.** Pressure curves for the HCCI engine experiment with gasoline at CR = 22.4—experimental results and simulations.

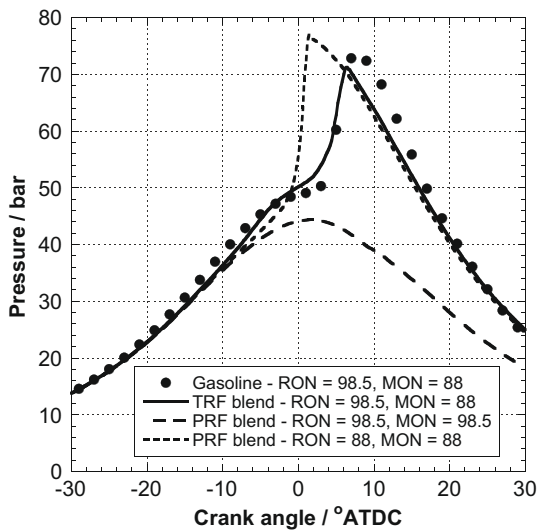


Fig. 14. Pressure curves for the HCCI engine experiment with gasoline at CR = 20 – experimental results and simulations.

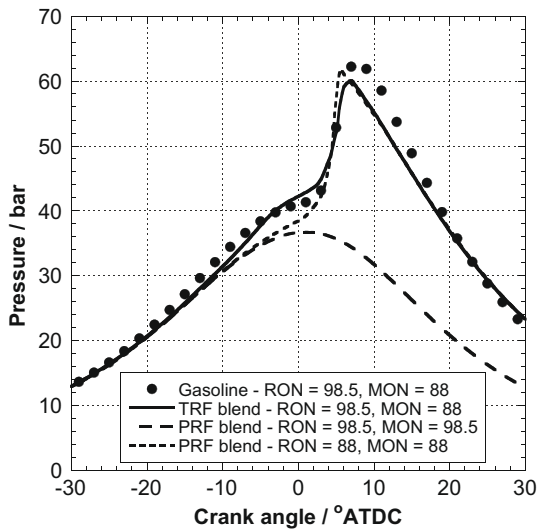


Fig. 15. Pressure curves for the HCCI engine experiment with gasoline at CR = 17.7 – experimental results and simulations.

its MON, implying that the  $K$ -value was around 1. This highlights the need for a surrogate fuel model that can accurately represent the differing resistances to auto-ignition that occur as engine conditions change.

## 5. Discussion

With significant research efforts being focused on understanding the oxidation of higher molecular mass liquid fuels [23,24], the impact of these collaborations on practical technologies will most likely come through improved chemical kinetic mechanisms. The possibility of full mechanisms for practical fuels, with or without additives, is unlikely to become a reality especially considering that these mechanisms would prove much too large to be of any practical use as within engineering tools such as 3D CFD. Furthermore, fundamental data of practical fuels such as flame speed and ignition delay times are not likely to be adopted as a metric of the quality of practical fuels in the same way that the RON and MON standards have been. As such the success of the uptake of new sur-

rogate mechanisms must come through the adoption of the octane numbers into the kinetic mechanism development process.

The presented methodology proposes a “second” generation of surrogate fuels to represent gasoline which adopts the practical standards – the road- and motor-octane numbers (RON and MON) – to dictate the composition of the surrogate blend. The example case of a 98.5 RON gasoline is that of a relatively high quality fuel, however equivalent blends can be formed for standard European gasolines and the “cheaper” grades of gasolines adopted in developing nations. By mapping the RON and MON for different TRF fuel blends, engineers now possess, for the first time, the ability to model different fuel grades. This also presents an opportunity for the simultaneous development of an engine and fuel together via computational modelling. This is of particular interest to those examining Premixed Charged Compression Ignition technologies where gasolines and blends of gasoline and diesel with lower RONs and MONs are proving more appropriate [25].

The study outlined here, links to the fundamentals of chemical kinetic mechanism development via the adoption of a stochastic reactor model to simulate engine combustion. By eliminating the complex engine combustion flow processes (adequate for HCCI) but still retaining mixture strength- and temperature-stratification, the full benefits of detailed mechanisms can be exploited. Benefits including improved robustness in terms of heat release rate and emissions calculations. Critically, when compared to conventional CFD, computations are completed in timescales (1 h) which are amenable to carry out optimisation and parametric studies. The latter are of particular importance when seeking subtle efficiency gains in engine performance for “blue-sky” development phases of projects such as searching for ideal fuelling choice and strategy.

The RON/MON test data have highlighted a number of interesting observations which require further thought. Firstly, the fact that TRFs do not blend in a linear manner is critical when employing this sort of methodology as small deviations in the calculation of RON and MON can lead to significantly different engine performance. This justifies these research efforts, and demonstrates its importance when considering the adoption of next-generation surrogate fuel models. Secondly, given that there are a number of TRF blends with equivalent RONs and MONs, a third metric should be employed to identify the most appropriate surrogate blend for improved fuel matching. The authors propose that this could either be that of closest flame speed, or in terms of most similar aromatic/paraffinic proportions. Indeed the former may well prove most appropriate for computations of SI combustion heat release, but the latter in terms of emissions such as soot where the toluene component can rapidly form benzene and other soot precursors.

Given the success of the proposed methodology for the simulation of HCCI combustion, this work has demonstrated that surrogate fuels can be used to emulate practical fuels when basing their composition on the practical fuel's more industrially-minded metrics.

## 6. Conclusions

A simple 2nd order polynomial was employed to map ternary compositions of toluene, i-octane and n-heptane into RON and MON space based on new experimental data for the octane numbers of these toluene reference fuels. This mapping was then inverted, allowing one to calculate the composition of surrogate blend according to the specified RON and MON of a real fuel.

The 2nd order response surface was found to be considerably more accurate than the standard linear-by-volume equations more commonly used. This implied that the blending of RON and MON are non-linear and consist of both synergistic and antagonistic regions, the latter being especially prevalent when blending toluene and i-octane together. The sources of these behaviour were identi-

fied using a modified sensitivity analysis to isolate the key reactions from a detailed chemical kinetic mechanism. The reverse mapping showed that it was possible for some blends to share the same RON and MON, suggesting that a third metric might be used to affix one to a particular blend. It was found that a TRF fuel, blended according to the mapping to match the RON and MON of a refinery gasoline with RON = 98.5 and MON = 88, accurately captured the main heat release event and pressure profile of the HCCI experiments using that gasoline. Two PRF fuels, blended to match the RON or MON were either too resistant or ignited too quickly.

The method outlined is not limited to TRF blends. As more components are added to surrogate fuels (ethanol and diisobutylene (DIB) [26] for example) the number of design points can be increased to incorporate the new dimensions, and the response surfaces can be adapted accordingly. There will also be scope to increase the number of metrics that the response surfaces approximate for. Not stopping at RON and MON, but adding flame speed, volatility, viscosity, smoke point, and a host of other physical properties that the real fuel may possess, and that modellers will wish to capture in their surrogate.

These results go some way to show that when considering the merits of a surrogate fuel for the modelling of gasoline, the ability to match the research octane- and motor-octane numbers simultaneously is of great importance.

## Acknowledgments

Neal Morgan would like to thank the European union for his funding under the European Commission Marie Curie Transfer of Knowledge Scheme (FP6) pursuant to Contract MTKI-CT-2004-509777 under the SUSTAINABLE FUELUBE project with Shell Global Solutions UK.

## References

- [1] Standard test method for research octane number of spark-ignition engine fuel, ASTM D2699-08.
- [2] Standard test method for motor octane number of spark-ignition engine fuel, ASTM D2700-08.
- [3] W. Leppard, The chemical origin of fuel octane sensitivity, SAE Paper No. 902137.
- [4] G. Kalghatgi, Auto-ignition quality of practical fuels and implications for fuel requirements of future SI and HCCI engines, SAE Paper No. 2005-01-0239.
- [5] J. Andrae, P. Björnbom, R. Cracknell, G. Kalghatgi, Autoignition of toluene reference fuels at high pressures modeled with detailed chemical kinetics, Combust. Flame 149 (1–2) (2007) 2–24.
- [6] J. Andrae, T. Brink, G. Kalghatgi, HCCI experiments with toluene reference fuels modelled by a semidetailed chemical kinetic mechanism, Combust. Flame 155 (4) (2008) 696–712.
- [7] R. Myers, D. Montgomery, *Response Surface Methodology*, Wiley Interscience, 2002.
- [8] M. Kraft, P. Maigaard, F. Mauss, M. Christensen, B. Johansson, Investigation of combustion emissions in a homogeneous charge compression injection engine: measurements and a new computational model, Symp. (Int.) Combust. 28 (1) (2000) 1195–1201.
- [9] M. Christensen, A. Hultqvist, B. Johansson, Demonstrating the multi fuel capability of a homogeneous charge compression ignition engine with variable compression ratio, SAE Technical Paper Series 1999-01-3679.
- [10] J. Pan, C.G.W. Sheppard, A. Tindall, M. Berzins, S.V. Pennington, J.M. Ware, End gas inhomogeneity, autoignition and knock, SAE Trans. 107 (1998) 1748–1762.
- [11] Automotive fuels – unleaded petrol – requirements and test methods, BSI BSI BS EN 228.
- [12] A. Burluka, K. Liu, C. Sheppard, A.J. Smallbone, R. Woolley, The influence of simulated residual and NO concentrations on knock onset for PRFs and gasolines, SAE Paper No. 2004-01-2998, 2004.
- [13] A. Bhave, M. Kraft, F. Mauss, A. Oakley, H. Zhao, Evaluating the EGR-AFR operating range of a HCCI engine, SAE Paper No. 2005-01-0161, 2005.
- [14] S. Mosbach, M. Kraft, A. Bhave, F. Mauss, J.H. Mack, R.W. Dibble, Simulating a homogenous charge compression ignition engine fuelled with a DEE/EtOH blend, SAE Paper No. 2006-01-1362, 2006.
- [15] H. Su, A. Vikhansky, S. Mosbach, M. Kraft, A. Bhave, K.-O. Kim, T. Kobayashi, F. Mauss, A computational study of an HCCI engine with direct injection during gas exchange, Combust. Flame 147 (1–2) (2006) 118–132.
- [16] S. Mosbach, H. Su, M. Kraft, A. Bhave, F. Mauss, Z. Wang, J.-X. Wang, Dual injection HCCI engine simulation using a stochastic reactor model, Int. J. Engine Res. 8 (1) (2007) 41–50.
- [17] S. Mosbach, A.M. Aldawood, M. Kraft, Real-time evaluation of a detailed chemistry HCCI engine model using a tabulation technique, Combust. Sci. Technol. 180 (7) (2008) 1263–1277.
- [18] A.M. Aldawood, S. Mosbach, M. Kraft, HCCI combustion phasing transient control by hydrogen-rich gas: investigation using a fast detailed-chemistry full-cycle model, SAE Paper No. 2009-01-1134, 2009.
- [19] J.E. Etheridge, S. Mosbach, M. Kraft, H. Wu, N. Collings, A detailed chemistry multi-cycle simulation of a gasoline fueled HCCI engine operated with NVO, SAE Paper No. 2009-01-0130, 2009.
- [20] S. Mosbach, M.S. Celnik, A. Raj, M. Kraft, H.R. Zhang, S. Kubo, K.-O. Kim, Towards a detailed soot model for internal combustion engines, Combust. Flame 156 (6) (2009) 1156–1165.
- [21] L. Cao, H. Su, S. Mosbach, M. Kraft, A. Bhave, Studying the influence of direct injection on PCCI combustion and emissions at engine idle condition using two dimensional CFD and stochastic reactor model, SAE Paper No. 2008-01-0021, 2008.
- [22] A. Smallbone, A. Bhave, N. Morgan, M. Kraft, R. Cracknell, G. Kalghatgi, Simulating combustion of practical fuels and blends for modern engine applications using detailed chemical kinetics, SAE Paper No. 2010-01-0572, 2010.
- [23] K.V. Puduppakkam, C.V. Naik, L. Liang, E. Meeks, B.G. Bunting, Combustion and emissions modeling of a gasoline hcci engine using model fuels, SAE Paper No. 2009-01-0669, 2009.
- [24] PrIMe Kinetics, <<http://www.primekinetics.org>>.
- [25] G. Kalghatgi, L. Hildingsson, B. Johansson, Low nox and low smoke operation of a diesel engine using gasoline-like fuels, in: Proceedings of the ASME Internal Combustion Engine Division 2009 Spring Technical Conference, Paper No. ICES2009-76034, 2009.
- [26] J. Andrae, R. Head, Hcci experiments with gasoline surrogate fuels modeled by a semidetailed chemical kinetic model, Combust. Flame 156 (2009) 842–851.
- [27] J. Heywood, *Internal Combustion Engine Fundamentals*, McGraw Hill, 1988.
- [28] G. Kalghatgi, P. Risberg, H.-E. Angstrom, A method of defining ignition quality of fuels in HCCI engines, SAE Paper No. 2003-01-1816.
- [29] G. Kalghatgi, B. Head, The available and required autoignition quality of gasoline-like fuels in HCCI engines at high temperatures, SAE Technical Paper Series 2004-01-1969.